DIFFERENT ASPECTS OF THE INTERFERENCES CAUSED BY WIND FARMS OVER TV SIGNALS

C. C. Alejandro [1] and C. R. Miguel[1], Leandro de Haro y Ariet[1], Pedro Blanco-González[2]

[1] *Dpto. de Señales, Sistemas y Radiocomunicaciones. Universidad Politécnica de Madrid*
ETSI de Telecomunicación. Ciudad Universitaria s/n. 28040 Madrid. SPAIN
{acalo, miguel, leandro}@gr.ssr.upm.es

[2] *Iberdrola S.A*
pedro.blanco@iberdrola.es

Abstract— **One of the environmental effects of wind farms is that wind turbines act as scattering devices of the electromagnetic RF waves and thus, may cause interferences to different telecommunication services around them. To carry on with a previous work [4], the model of the nacelle and the wind turbine is shown and validated. Finally, a wideband terrain-sensitive channel response model has been developed from narrow-band model. The complex wideband channel transfer function is transformed here to the time domain through the use of a fast Fourier transform (FFT), so that calculating the power delay profile (PDP)**

I. INTRODUCTION

Nowadays, wind power is one of the more important renewable energy sources (it allows a sustainable exploitation of the resources with relatively low costs). Compared to the environmental effects of traditional energy sources, the environmental effects of wind power are relatively minor. Wind power consumes no fuel, and emits no air pollution, unlike fossil fuel power sources [2].

Despite its high profitableness and low environmental effects, planned wind turbines or wind farms have to be approved by building authorities on the base of statements of system providers which may run systems. For that, safeguarding zones are intended to be defined on the basis of the predicted distortions [3].

In this paper, the interference caused by wind farms over the broadcast TV service will be analyzed. Wind turbines act as scattering devices of the electromagnetic RF waves, producing signal echoes. These echoes potentially degrade the TV signal reception.

This phenomenon on analogical TV has been studied by the ITU that established the recommendation ITU-R BT. 805 .This recommendation gives a method to determine the delay and the interference requirements from a single turbine to obtain a good quality analog TV reception.

II. SCATTERING MODEL

An essential element in considering the effect of a wind turbine over the TV signal is the strength of the reflection from the turbine. This is measured by its RCS, which is an area, usually measured in square meters.

It is known and a well established fact [1] that the Radar Cross Section RCS is defined for plane wave excitation only. The limit condition R implies that explicitly.

$$\sigma = \lim_{R\to\infty} 4\pi R^2 \frac{\|E_s\|^2}{\|E_i\|^2} \qquad (1)$$

In order to estimate de RCS of a wind turbine the full turbine is modeled as a set of sections or scattering centers.

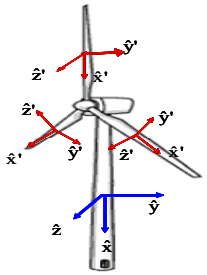

Fig. 1: Main Scatter centers of a wind turbine.

In a previous work [4], a scattering model of the blades and the tower of a wind turbine was developed. In this section a physical optics based model of a nacelle is shown. This one has been considered as a metallic rectangular box where each face is modeled like a different scattering centre. The shadowing effect (which depends on the incidence direction) among the scattering centers has been taken into account.

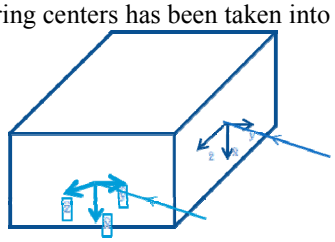

Fig. 2: Model of a nacelle

The RCS has been calculated from the sum of the field scattered by each of them, taken into account their phase shifted.

The Fig. 3 shown a comparison between the theoretical RCS values of a nacelle of 15x5x5 m^3 and that obtained from the simulating software Feko. The RCS has been studied for two different incidence directions: $\theta_i = 30$ and $\theta_i = 60$, and

for the scattering plane $\phi_s = 90$. It can be observed the good agreement between both results.

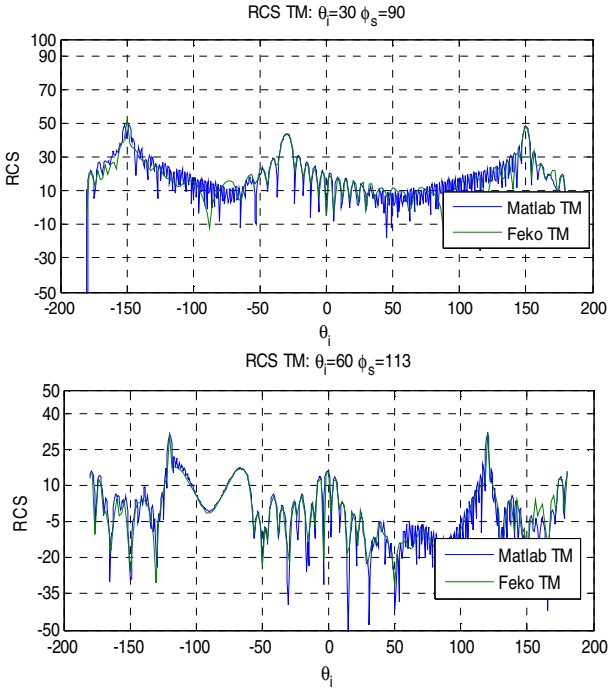

Fig. 3: Theoretical versus simulated bistatic RCS values.

From the models of the different parts of a wind turbine is possible to obtain its RCS according to the following equation:

$$\sigma = \left| \sum_{i=1}^{N} \sqrt{\sigma_i}\, e^{-j\beta(-\hat{r}_{inc}\cdot\vec{d}_i + \hat{r}_s\cdot\vec{d}_i)} \right|^2 \qquad (2)$$

To validate the full model, the theoretical RCS values of a wind turbine have been compared with that accomplished with the software Feko. The used wind turbine had a tower 80m high and blades 40m long (the nacelle had the same size than the previous one).

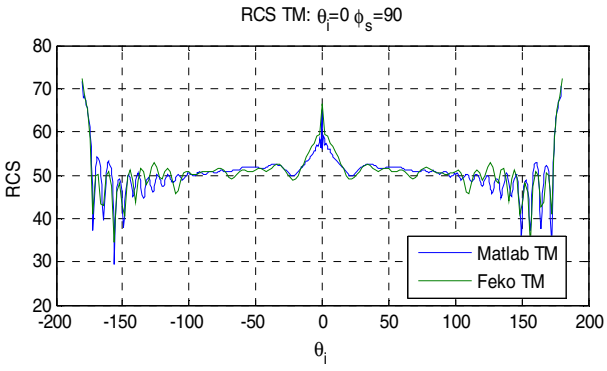

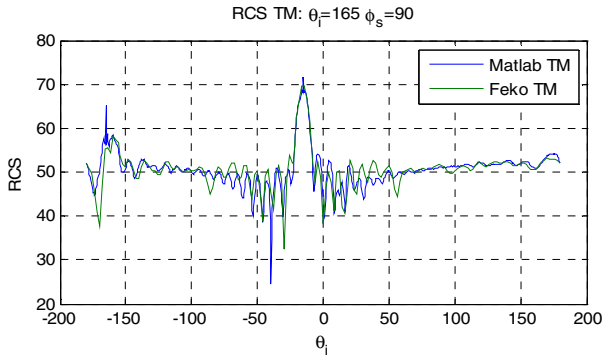

Fig. 4: Theoretical versus simulated bistatic RCS values of a wind turbine

III. 3D Scattering Model

In order to obtain a more accurate value of the RCS of wind turbine it requires detailed geometry information so that a computer aided design (CAD) model of the turbine was created. Also required are the electrical properties of the construction materials if not made from metal.

Two CAD model was designed, one of them with a curved nacelle and the other one with a rectangular nacelle. They were compared with a theoretical model.

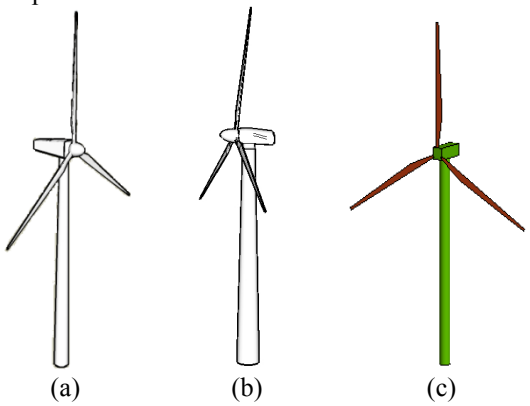

Fig. 5: Rectangular (a), curved (b) 3D model and theoretical (c) model.

Next, a comparison between the main scattering centers and the full models of a wind turbine will be shown. The models have blades 38m long, nacelles 15m long x 15m wide and tower 72m long with 3m radius. The incidence direction of the plane wave is normal to the blade surface and its frequency is 827MHz.

In the Fig. 6, the full RCS of each model is shown. As we can see, the theoretical model presents a greater RCS outside the forward direction. It is due to the high level of RCS of the theoretical tower respect to the other ones. The strengths of the RCS in the forward direction are similar because the forward scattered lobe for any obstacle is proportional to its projected area [8].

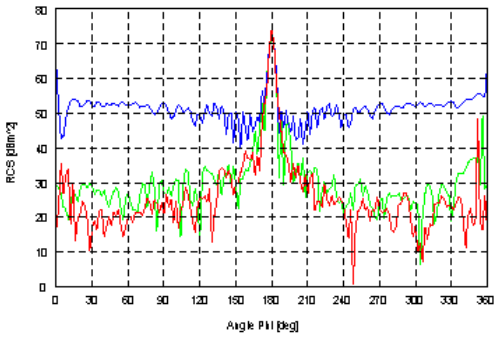

Fig. 6. Bistatic RCS comparison between 3D and theoretical models: theoretical model (blue), rectangular model (red) and curved model (green).

Next, the comparison among the RCS of the blades shown in Fig. 7 reveals how the strengths of the RCS in the forward direction are also similar and both curves have the same way for the directions between 150º and 180º, due to triangular shape of the blade. The differences in the rest of the diagram can be caused, partly, by the 3D profile of the blade in contrast to the 2D profile of the theoretical one.

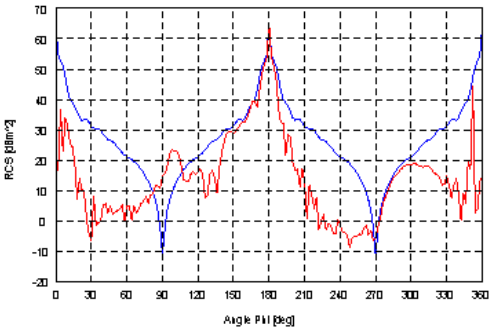

Fig. 7. Bistatic RCS comparison between 3D and theoretical blades: theoretical model (blue) and 3D model (red).

Like the previous comparisons, in the case of the tower, the strength of the RCS in the forward direction is the same, but outside of this direction the theoretical RCS is much greater than those of the 3D models. The reason for that, partly, is that the shape of the 3D tower is really a cone, with different radii values in each ends.

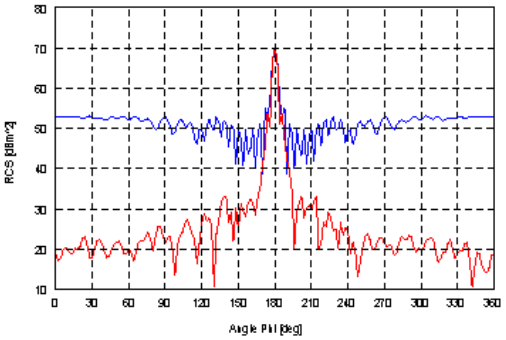

Fig. 8. Bistatic RCS comparison between 3D and theoretical tower: theoretical model (blue) and 3D model (red).

With respect to the RCS of the three types of nacelles, the Fig. 9 shows the well agreement between the specular and forward lobe of the rectangular (blue) and theoretical nacelle (green).

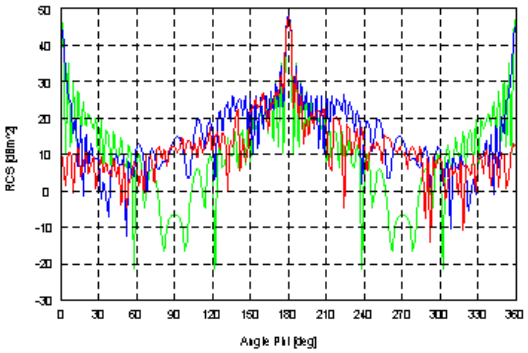

Fig. 9. Bistatic RCS comparison between 3D and theoretical nacelles: theoretical (green), rectangular (blue) and curved (red).

IV. SPECTRAL CONTENT OF THE RCS

Because of the movement of the blades, the scattered electric field and the RCS of the wind turbine have time variations. If we suppose time-harmonic electromagnetic fields then [6]:

$$\vec{E}(r,t) = Re\left(\vec{E}(r)e^{jw_o t}\right) = \\ = \frac{1}{2}\left[\vec{E}(r)e^{jw_o t} + \vec{E}(r)^* e^{-jw_o t}\right] \quad (3)$$

$$\vec{S}(r,t) = \frac{1}{2}\left[Re\left(\vec{E}(r)x\vec{H}(r)^*\right) = \\ = +Re\left(\vec{E}(r)x\vec{H}(r)e^{-j2w_o t}\right)\right] \quad (4)$$

Since both E and H are not functions of time and the time variations of the second term are twice the frequency of the field vectors, the time-average Poynting vector (average power density) over one period is equal to:

$$\vec{S}_{average}(r) = \vec{S} = \frac{1}{2}Re\left(\vec{E}(r)x\vec{H}(r)^*\right) \quad (5)$$

The average power density scattered by a wind turbine can be expressed like:

$$\vec{S}_{scatt}(r) = \frac{S_i \cdot \sigma}{4\pi R^2} \quad (6)$$

It causes that the mean value and the standard deviation of the strength of the received electric field change during one full turn.

This temporal oscillation has associated a spectral content related with the size of the blades and the angular velocity (Doppler effect). The spectra have been calculated using a complete revolution of the rotor, so it shows the frequency content averaged over the whole cycle. We expect to see negative and positive frequency components for parts of the cycle when a blade is moving towards and away from the direction of incidence. The maximum significant frequency component should match up to the blade tip speed. The RCS for different position of the blades has been obtained with Feko software.

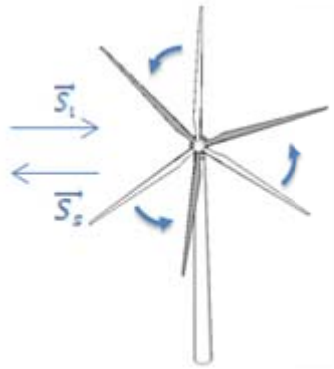

Fig. 10. Turn of the blades and scattered field.

Simulated values, including both the effect of the blades and the tower can be seen in

Fig. 11.When the blades are rotating in a plane containing both direction of incidence and turbine, we obtain the "worst case" from the viewpoint of the magnitude of the return. In the next figure, the blue curve represents the RCS taken into account the blades and the statics parts of the wind turbine, whereas in the green one the static parts have been eliminated (DC level).

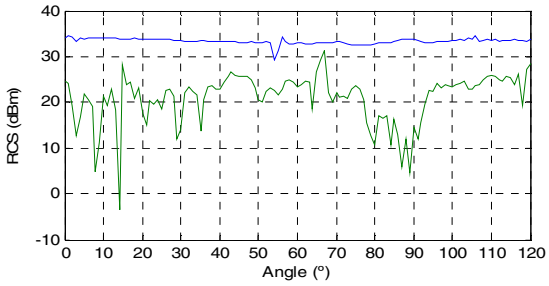

Fig. 11. RCS time variations due to the movement of the blades.

The Fig. 12 shows the discrete Fourier transform (obtained through FFT algorithms) of the temporal values of the RCS. The wide of the spectral content is 140 Hz which according to the Doppler frequency deviation corresponds to a blade tip speed of 25m/s (fo=827MHz). In the 3D models, the blades are 38m long and the angular velocity is 120º/s, so the maximum speed would be about 80m/s. This difference can be due to the fact that the edges of the blades not lie fully in the incidence plane.

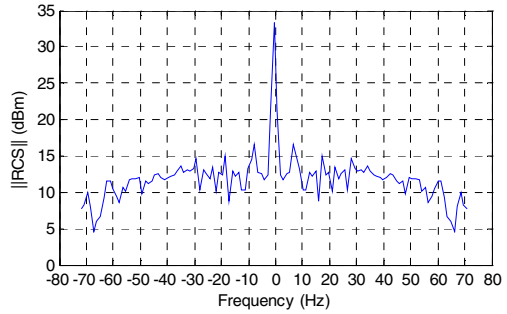

Fig. 12. Spectral content of the RCS.

V. Wideband Power Delay Profile (PDP)

In a previous work [4], the validation of the computer model was done estimating a narrow band PDP. The theoretical channel transfer function was obtained based on only one frequency value, "fo". In this work, the received signal has been modelled as the sum of several echo signals.

$$Y(r,f) \overset{\text{def}}{=} E_{TOT}(r,f) = \\ = \sum_{i=1}^{Ntu} |E_i(r,f)| e^{-j2\pi f \tau_i} \delta(f-f_o) + |E_c(r,f)|\,\delta(f-f_o) \quad (7)$$

The channel response can be calculated from the free space channel response (isotropic transmitting and receiving antennas) and received signal as:

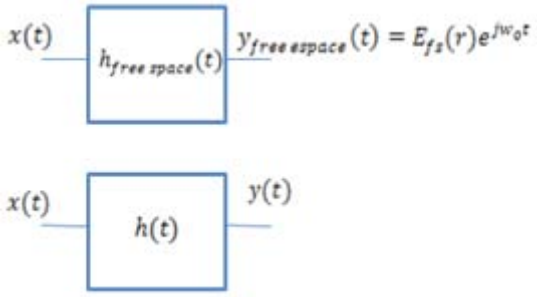

Fig. 13. Relation between any channel response and the free channel response.

$$H(r,f) = \frac{Y(r,f)}{Y_{fs}(r,f)} H_{fs}(r,f) = \\ = \frac{\lambda}{4\pi R \cdot |E_{fs}(r)|} \sum_{i=1}^{Ntu} |E_i(r,f)| e^{-jw\tau_i} + |E_c(r,f)| \quad (8)$$

$$\left\| H_{fs}(r,f) \right\|^2 = \left(\frac{\lambda}{4\pi R} \right)^2 \quad (9)$$

$$Y_{fs}(r,f) \overset{\text{def}}{=} \underset{fs}{E_{TOT}} = |E_{fs}(r)| \delta(f-f_o) \quad (10)$$

$$|E_{fs}(r)| = \frac{\sqrt{30 \cdot P_{TX}}}{R} \quad (11)$$

The amplitude of the electric field of each received echo was calculate making use of the ITU P.1546 Recommendation (which takes into account the orographic profile) and the phase information was estimated from the frequency "fo" and the distance among transmitter – wind turbine – receiver. In narrow band model, the channel response is almost plane around the frequency band of the input signal, for that reason we can suppose that the spectral content of the channel response is constant and the time channel response is a set of "delta" functions.

$$H(r,f) = \frac{\lambda}{4\pi \cdot |E_{fs}(r)|} \cdot \left(\sum_{i=1}^{Ntu} |E_i(r)| e^{-jw\tau_i} + |E_c(r)| \right) \quad (12)$$

$$h(t) = \frac{\lambda}{4\pi \cdot |E_{fs}|} \cdot \left(\sum_{i=1}^{Ntu} |E_i(r)| \delta(t-\tau_i) + |E_c(r)|\,\delta(t) \right) \quad (13)$$

This hypothesis is true when the bandwidth of the input signal is lower than the inverse of the maximum delay of the channel [7].

$$\frac{1}{\tau_{max}} \geq W \qquad (14)$$

In our case, where the bandwidth of a TV channel is about 8MHz and the maximum delay of the channel due to multipath is greater than 8us, it is necessary to study wideband radio-channel propagation characteristics. Computation of the wide-band complex channel transfer function is accomplished by making discrete frequency calculations using the previous narrow band model across the desired RF bandwidth.

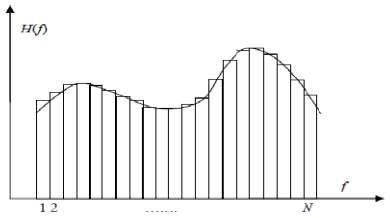

Fig. 14. Wideband channel response from narrow band models.

This transfer function can then be used to give an estimate of the low-pass equivalent bandpass impulse response of the channel. This is possible since the phases as well as the amplitude of the field are known. From the low-pass equivalent response is possible to obtain the PDP of the bandpass channel according to:

$$h(t) = Re\left(\hat{h}(t)e^{j2\pi f_c t}\right) \qquad (15)$$

$$PDP(t) \stackrel{\text{def}}{\equiv} \left\|\hat{h}(t)\right\|^2 \qquad (16)$$

The time/frequency relationships used in simulating the wideband response are as follows: maximum delay equal to 8us; 64-FFT and sample frequency equal to 8MHz (the bandwidth of the low-pass equivalent of a TV channel is 4MHz).

The Fig. 15 shows wide band Power Delay Profile for a typical wind farm scenario.

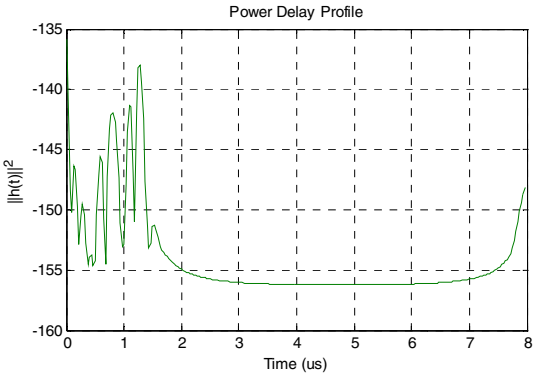

Fig. 15. Wideband PDP.

The wideband channel takes into account the interference between echoes that arrives in different moments.

VI. Conclusions

In this work a scattering model for a nacelle have been proposed and validated with results obtained by simulation software (Feko). From the scattering model of the scattering centers of a wind turbine we have obtained its RCS which also was validate with Feko software. Finally, the wideband power delay profile of the propagation of the TV signals over a wind farm has been estimate.

VII. Future Work

In order to analyse the DVB-T signal received by a TV receiver in presence of a wind farm, a model of transmitting and receiving chain will be developed (OFDM transmission and reception).

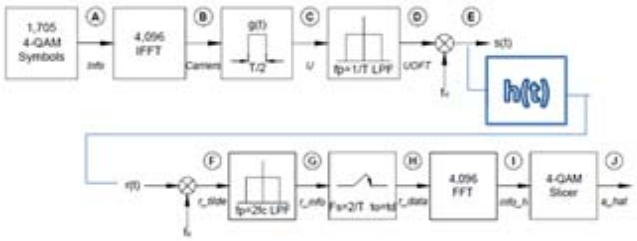

Fig. 16. Transmitting and receiving chains of a DVB-T signal.

References

[1] IEEE STD 211-1997, Definition of terms

[2] http://www.sustainabilitycentre.com.au/WindPowersStrength.pdf

[3] Gerhard Greving, "*Weather Radar and Wind Turbines – Theoretical and Numerical Analysis of the Shadowing Effects and Mitigation Concepts*", The Fifth European Conference On Radar In Meteorology And Hydrology, ERAD 2008.

[4] A. Calo, M. Calvo, L. de Haro and P. Blanco, "S*cattering Analysis of a Wind Farm*", The 20th International Zurich Symposium on Electromagnetic Compatibility, Zurich, January, 2009.

[5] ITU-R BT 805 "Assessment of impairment caused to television reception by a wind turbine"

[6] C. A. Balanis, "*Advanced Engineering Electromagnetics*", J. Wiley & Sons 1989.

[7] R. J. Luebbers, W. A. Foose, and G. Reyner, "*Comparison of GTD propagation model wide-band path loss simulation with measurements*,"IEEE Trans. Antennas Propagat., vol. 37, pp. 499–505, Apr. 1989.

[8] E.F. Knott et.al, "*Radar Cross Section*", Artech House, London 1992